Calcium Channel Antagonists Discovered by a Multidisciplinary Approach

Emanuele Carosati,[†] Gabriele Cruciani,*[,†] Alberto Chiarini,[‡] Roberta Budriesi,[‡] Pierfranco Ioan,[‡] Raffaella Spisani,[§] Domenico Spinelli,[§] Barbara Cosimelli,[∥] Fabio Fusi,[⊥] Maria Frosini,[⊥] Rosanna Matucci,[#] Francesco Gasparrini,[▽] Alessia Ciogli,[▽] Philip J. Stephens,[○] and Frank J. Devlin[○]

Dipartimento di Chimica, Università degli Studi di Perugia, Via Elce di Sotto 10, 06123 Perugia, Italy, Dipartimento di Scienze Farmaceutiche, Università degli Studi di Bologna, Via Belmeloro 6, 40126 Bologna, Italy, Dipartimento di Chimica Organica "A. Mangini", Università degli Studi di Bologna, Via S. Giacomo 11, 40126 Bologna, Italy, Dipartimento di Chimica Farmaceutica e Tossicologica, Università degli Studi di Napoli "Federico II", Via Montesano 49, 80131 Napoli, Italy, Dipartimento di Scienze Biomediche, Università degli Studi di Siena, Via A. Moro 2, 53100 Siena, Italy, Dipartimento di Farmacologia Preclinica e Clinica, Università degli Studi di Firenze, Viale Pieraccini 6, 50139 Firenze, Italy, Dipartimento di Studi di Chimica e Tecnologia delle Sostanze Biologicamente Attive, Università "La Sapienza", Piazzale A. Moro 5, 00185 Roma, Italy, and Department of Chemistry, University of Southern California, Los Angeles, California 90089-0482

Received April 12, 2006

A multidisciplinary project has led to the discovery of novel, structurally diverse, L-type calcium entry blockers (CEBs). The absolute configuration of a recently reported CEB has been determined by vibrational circular dichroism spectroscopy, to assign the stereospecificity of the ligand−channel interaction. Thereafter, a virtual screening procedure was performed with the aim of identifying novel chemotypes for CEBs, starting from a database of purchasable compounds; 340 000 molecules were screened *in silico* in order to prioritize structures of interest for bioscreening. As a result, 20 compounds were tested in vitro, and functional and binding assays revealed several hits with promising behavior as CEBs.

Introduction

Calcium antagonists are important cardiovascular drugs currently in use in the treatment of hypertension and angina pectoris.[1] Their pharmacological effect is due to the selective inhibition of the influx of extracellular calcium through L-type voltage-operated calcium channels.[2]

The terms calcium channel blockers (CCBs) and calcium entry blockers (CEBs) are currently used to define three major classes of antagonists.[3] The most studied class of antagonists is the 1,4-dihydropyridines and the second class is the phenylalkylamines, whereas the third and structurally distinct class is the benzothiazepines, represented by diltiazem (DTZ). Phenylalkylamines and benzothiazepines bind to a site on the calcium channel that is allosterically linked to the dihydropyridines receptor.[4]

Diltiazem is one of the most important calcium channel blocking agents in clinical use for the treatment of angina and hypertension.[1,6] However, it has a relatively short duration of action, and it is known to cause significant prolongation of cardiac PR intervals[7] and to potently inhibit the metabolism of a variety of co-administered drugs,[8] often resulting in increased plasma concentrations and/or severe toxicity.

The collection of diltiazem analogues is limited[9−11], and little information has been available on their binding mode or structure−activity relationships (Chart 1). Similarity to diltiazem was postulated for a new series of calcium antagonists; the oxadiazol-3-one derivatives recently synthesized exhibited very interesting negative inotropic potency.[12] In this context, a series of acetals was designed and functionally assayed, and the series of oxadiazolones was optimized with an ethyl group at position 8 (8-(4-bromophenyl)-8-ethoxy-8*H*-[1,4]thiazino[3,4-*c*][1,2,4]-oxadiazol-3-one, coded as **5b**).[13]

Chart 1. Diltiazem and Some Other Structurally Related Calcium Antagonists

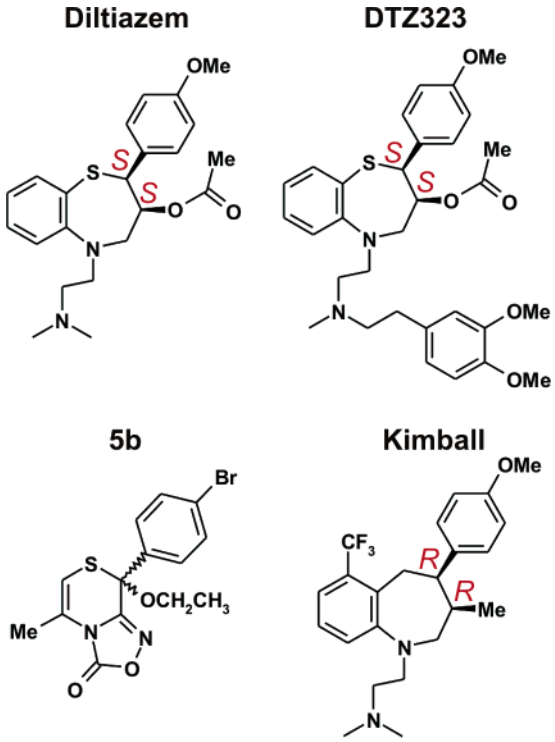

However, important questions remained unsolved. Does **5b** bind at the diltiazem binding site or does it have its own site? Are both enantiomers of **5b** active, or is only a single enantiomer active? Could **5b** be used as a new template to search for novel

* To whom correspondence should be addressed. Tel: +39 075 585 5550. Fax: +39 075 45646. E-mail: gabri@chemiome.chm.unipg.it.
[†] Università degli Studi di Perugia.
[‡] Dipartimento di Scienze Farmaceutiche, Università degli Studi di Bologna.
[§] Dipartimento di Chimica Organica "A. Mangini", Università degli Studi di Bologna.
[∥] Università degli Studi di Napoli "Federico II".
[⊥] Università degli Studi di Siena.
[#] Università degli Studi di Firenze.
[▽] Università "La Sapienza" Roma.
[○] University of Southern California.

10.1021/jm0604373 CCC: $33.50
Published on Web 07/27/2006

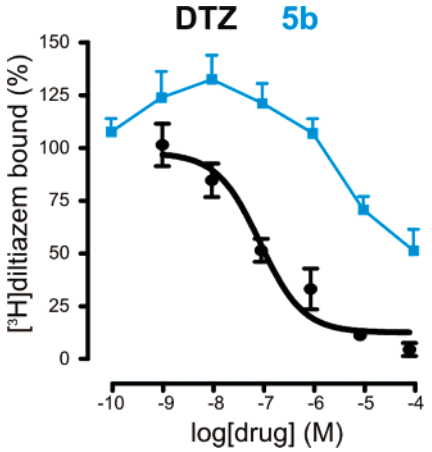

Figure 1. Effects of **5b** and **DTZ** on [^{3}H]diltiazem binding.

calcium antagonists? We attempt to answer these relevant questions in this article.

First, assays on rat cardiomyocites with [^{3}H]diltiazem as the radioligand were performed, and the direct interaction at the diltiazem binding site was confirmed for **5b**, although only at high concentrations. In addition, for **5b**, the (−) isomer exhibited a more noticeable negative inotropic activity, demonstrating the stereospecificity of the binding site.

Then, a ligand-based virtual screening (LBVS) procedure was developed in order to search for novel chemotypes for CEBs, starting from the oxadiazolone series, and shed light on the binding mode of this interesting series of modulators. Compound **5b** was used as the structural query, and a virtual library of purchasable molecules was reduced to a smaller set, enriched in potential hits. The characterization of the most active oxadiazolones, the computational procedure for the screening, and the biological evaluation of the selected compounds are described in this article.

Results and Discussion

Characterization of Oxadiazolones. Binding Profile. Equilibrium saturation experiments demonstrated that cardiac sarcolemmal membrane binds [^{3}H]diltiazem with a dissociation constant (K_d) of 108 ± 19.2 nM and a maximal receptor density (B_{max}) of 1.4 ± 0.1 pmol/mg protein. The effect of compound **5b** displayed a complex interaction, with the binding of [^{3}H]-diltiazem either stimulated or inhibited at low (0.1 nM−1 μM) or high (10−100 μM) concentrations, respectively. Interestingly, a similar profile already observed for CEBs such as dihydropyridines, might reflect a positive allosteric modulation at the diltiazem binding site, which, at higher concentrations, turned into a direct and negative interaction.[14] The comparison of the effects of **5b** and **DTZ** on [^{3}H]diltiazem binding is graphically given in Figure 1.

Enantiomeric Separation. To evaluate the stereoactivity of **5b**, the two enantiomers were resolved by semipreparative enantio-HPLC obtaining, for each enantiomer, 11 mg with an e.e. of 99% (+) and 94% (−). Experimental details are reported in Figure 2. Additional experimental details (semipreparative and complete analytical conditions) are provided in the Experimental Section.

Absolute Configuration Assignment. The absolute configuration of **5b** was assigned using vibrational circular dichroism (VCD) spectroscopy.[15] The experimental IR and VCD spectra of (+)-**5b** are shown in Figure 3a. The VCD of **5b** is predicted using density functional theory (DFT).[15] **5b** is a conformationally flexible molecule. The relative energies and free energies

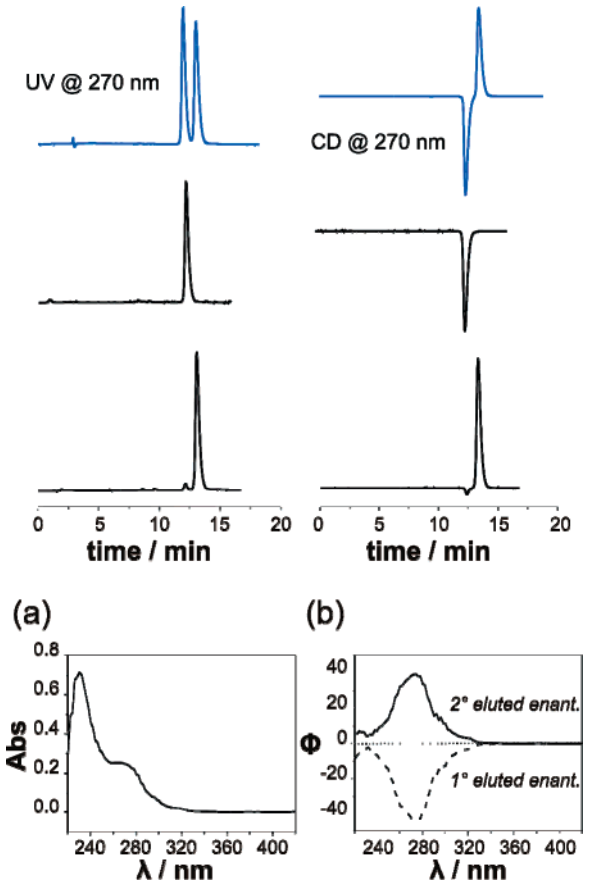

Figure 2. Analytical separation of the enantiomers of **5b** by enantioselective HPLC (chiral column (*R*,*R*)-DACH-DNB, I.D. 250 × 4.6 mm, flow rate 1 mL/min, T 25 °C, UV (left), and CD (right) detections at 270 nm). Top traces: racemic sample; middle and bottom traces: peak purity check of the pooled fractions (~11 mg) containing (−) and (+) enantiomers, respectively, after semipreparative HPLC. (a) on-line UV spectrum of **5b**; (b) on-line CD spectra of **5b** enantiomers.

and the resulting room-temperature equilibrium populations of the stable conformations calculated at the B3PW91/TZ2P level are detailed in the Supporting Information. The conformationally averaged B3PW91/TZ2P VCD spectrum of *S*-**5b** is compared to the experimental spectrum of (+)-**5b** in Figure 3b. The agreement of calculated and experimental VCD spectra is excellent and shows that the absolute configuration of (+)-**5b** is unambiguously *S*. It follows that the absolute configuration of the biologically active enantiomer, (−)-**5b**, is *R*. This conclusion is further supported by DFT calculations of the specific rotation, $[\alpha]_D$, and the electronic CD of **5b**, which will be reported elsewhere.

Virtual Screening Procedure. The affinity of compound **5b** with the diltiazem site at high concentration and the stereospecificity of its interaction with the calcium channel have shed more light on this interesting series of calcium antagonists. A novel approach to gain wider information was applied, and the virtual screening procedure was based upon the oxadiazolone **5b**.

The term virtual screening (VS) summarizes various computer-based methods developed for the selection of potential drug candidates from a large set of molecular structures. In situations where structural information about the protein target is available, more success could arise because of the knowledge of the binding site (structure-based virtual screening). In contrast, when just a few active compounds represent all of the available information, only similarity criteria among the query compounds and molecules from a database allow the database to be ranked.

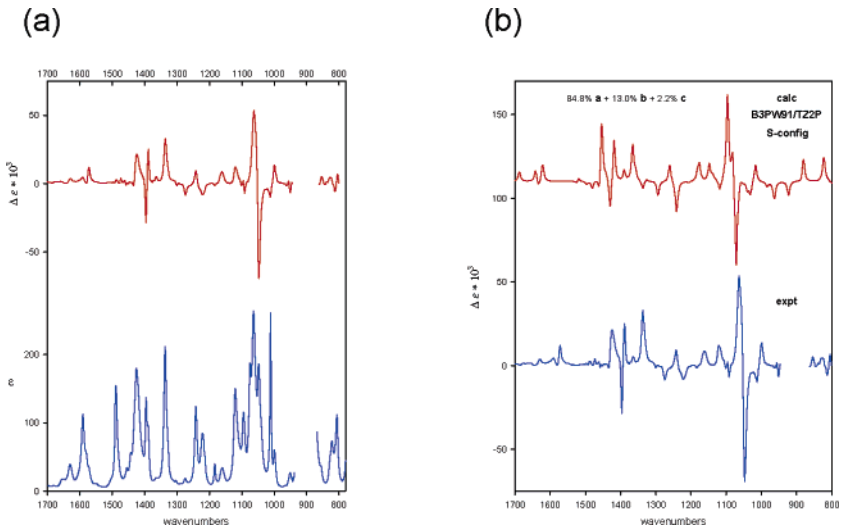

Figure 3. (a) Experimental IR and VCD spectra of (+) oxadiazol-3-one **5b** (0.04 M in $CDCl_3$). (b) Comparison of the B3PW91/TZ2P calculated VCD spectrum of *S*-**5b** and the experimental VCD spectrum of (+)-**5b**.

Table 1. Details regarding the Vendors[17]

company code	compds	company name	company website
Aldrich	198160	Sigma-Aldrich, Inc.	http://www.sigmaaldrich.com
Bionet	47401	Key Organics, Ltd.	http://www.keyorganics.ltd.uk
Maybridge	83286	Maybridge Chemicals	http://www.maybridge.com
Menai	5017	Menai Organics, Ltd.	http://www.ryansci.com
Peakdale	8548	Peakdale Molecular	http://www.peakdale.co.uk
overall	342412		

The highest ranked molecules are expected to behave in a manner similar to that of the query compounds because it is assumed that molecules with similar features exhibit similar biological activity.

A database of approximately 340 000 commercially available compounds was assembled in-house from commercial catalogues (the molecules were downloaded as either multi-mol2 or SD files)[16] to search for new chemotypes by means of a LBVS procedure; details on vendors are summarized in Table 1. The screening described below is composed of a cascade of *in silico* filters as summarized in Figure 4.

The database was cleaned up at the earliest stage because all subsequent steps rely on the quality of the chemical structures. The structures of all of the molecules of the dataset were directly provided by vendor databases. In this first refinement, duplicates as well as salts and non covalent complexes were removed, and the chemical space was restricted to compounds with only C, H, N, O, S, P, and halogens, consistent with a great majority of drugs and drug-like molecules.[17] A total of about 240 000 compounds, approximately 70% of the initial amount, were retained. Next, a filter based on molecular weight (MW) was applied and the available chemical landscape reduced to about 157 000 compounds.

Afterward, the active *R*(−)-isomer of compound **5b** was chosen as the molecular template for a similarity filter. A pharmacophore was built upon compound **5b** using the novel computational procedure FLAP, which has been used to describe, in terms of pharmacophoric fingerprints, both ligands and proteins.[19] The molecular template served as the query to search the refined database. The similarity was based on the matching of pharmacophoric features between every dataset compound and the molecular template. The FLAP program identifies all of the ways in which four atoms of the test molecule can be paired to four corresponding atoms of the template.[18] The amount of common potential pharmacophores, filtered by molecular shape, gives back the similarity between the test molecule and the template.

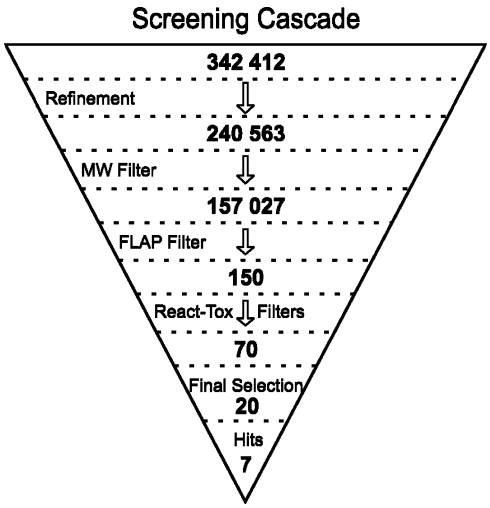

Figure 4. Screening cascade. The steps of the screening procedures are summarized. The first refinement and the filter on molecular weight cut about 50% of the initial compounds; with the FLAP similarity filter, the dataset was strongly reduced because only 1 out of 1000 was selected and further analyzed. Only 20 virtual hits constituted the final selection. See part D of the Experimental Section for details.

According to these similarity scores, all dataset compounds were ranked. Then, only the 150 best ranked virtual hits were extracted and further analyzed *in silico* according to the toxicity and reactivity of their chemical groups.[19,20] The removal of toxic or unstable compounds resulted in a list of 70 compounds. Out of these, only 20 representative virtual hits were selected for purchasing. Details for all of the filters used in the screening are given in the Experimental Section.

Chemical Profile of Virtual Hits. Among the virtual hits selected, five were purchased from Sigma-Aldrich, R59,053−3 (**A2**), R53,650-4 (**A3**), R70,210-2 (**A4**), R57,505-4 (**A5**), R53,643-1 (**A6**); five from Bionet, 9D-011 (**B2**), 8J-901 (**B3**), 3J-925 (**B4**), 12H-911 (**B5**), 3M-575S (**B6**); eight from Maybridge, CD 11279 (**M1**), SPB 06193 (**M2**), CD 08165 (**M3**), DP 01325 (**M4**), KM 05893 (**M5**), SEW 05125 (**M6**), S 12274 (**M7**), CD 10415 (**M8**); and one from Menai Organics, ST1749 (**Me**) and Peakdale, PFC-1390 (**P1**).

Chart 2. Structures of Compounds Identified Using Virtual Screening[a]

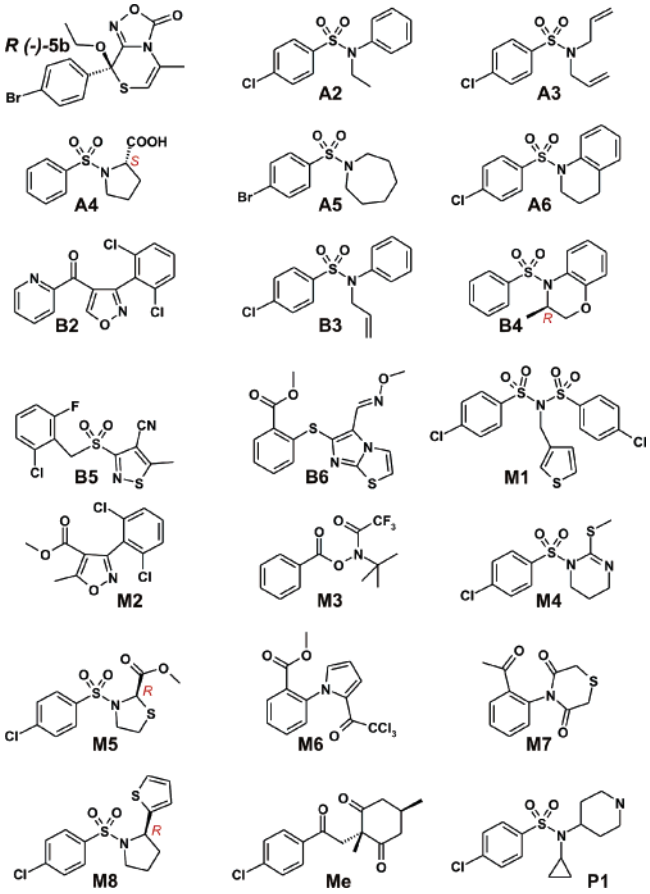

[a] Compounds coded with **A** as the first letter were purchased from Sigma-Aldrich, compounds with **B** were purchased from Bionet, and compounds with **M** were purchased from Maybridge, whereas compounds **Me** and **P1** were purchased from Menai Organics and Peakdale, respectively. Compounds **B4**, **M5**, and **M8** were purchased as racemates, and compound **A4** is *S*, whereas for **Me**, a mixture of cis/trans isomers was purchased. However, the computational procedure identified the stereoisomers reported as hits.

The structures of the selected compounds are shown in Chart 2. They exhibited some common scaffolds, and in particular, benzenesulfonamides were prominent. A high percentage of benzenesulfonamides was observed among the best-ranked compounds and was maintained in the final selection. The phenyl ring is *p*-substituted with chlorine, with few exceptions such as the unsubstituted phenyl ring (**B4** and **A4**) and the bromine in place of chlorine (**A5**). The substitution at the nitrogen varies within the set. Single substituents, which include the sulfonamide nitrogen, can be large and lipophilic, such as for **A5**, **A6**, **M8**, and **B4**, but they can also be less lipophilic, such as **A4**, **M4**, and **M5**. Among the remaining sulfonamides, **M1** is far different from the set because of the presence of two sulfonyl groups; simple lipophilic substituents, such as ethyl, allyl, and phenyl, are combined in **A2**, **A3**, and **B3**, whereas in **P1** the presence of piperidine and its basic nitrogen is noteworthy.

Different scaffolds constitute the remaining virtual hits. Similarities are rare, for example, **B2** and **M2**; all of the remaining compounds are structurally unique.

In this manner, a large chemical landscape has been investigated, and their 3D similarity was calculated toward query **5b**.

Functional Profile of Virtual Hits. The pharmacological profile of all 20 compounds was tested on guinea-pig isolated left and right atria to evaluate their inotropic and chronotropic effects, respectively, and on K^+-depolarized (80 mM) guinea-pig aortic strips to assess vasorelaxant activity. Data are reported in Table 2, together with those of reference compounds **DTZ** and **5b**.

While **DTZ** is characterized by negative inotropy and chronotropy as well as significant vasorelaxant activity, reference compound **5b** expressed only the negative inotropic effect, the *R*(−)-isomer being responsible for the majority of the activity.

Surprisingly, all of the selected compounds were found to have some inotropic activity, although all were at least 10-fold less potent than **5b**, the only oxadiazolone with negative inotropic potency in the nanomolar range. A very low potency was revealed for a few compounds, and a significant potency for a larger number of compounds, which were considered as hits.

Six out of 20 compounds, that is, 30% of the selected compounds, revealed a good inotropic profile, with negative inotropic EC_{50} values between 0.2 and 0.4 μM. They vary from the thiomorpholine-3,5-dione scaffold of **M7** to the benzenesulfonamide of all of the remaining compounds, which vary in the substitution at the nitrogen. It seems that at least one bulky and lipophilic group is necessary for negative inotropic activity. It can be either the phenyl of **A2**, **B3**, and **M7**, the azepine ring of **A5**, the 2-thienyl-pyrrolidine of **M8**, or the cyclopropyl in tandem with the 4-piperidinyl substituent of **P1**. This basic group also assigns a unique character to **P1**, the most promising hit of the series. An example of the decrease in developed tension is provided for **P1** in Figure 5.

Six other compounds revealed an inotropic potency of the same magnitude as that of the reference **DTZ**. The absence of *p*-chlorine as well as the presence of oxygen in the ring makes the structure of **B4** unique within the benzenesulfonamide series. Similarly, compound **B6** is almost unique because of its S-bridge and imidazo[2,1-*b*]thiazole ring, whereas compounds **B2** and **M2** as well as compounds **A4** and **M5** can be paired.

All of the remaining compounds have very low negative inotropic potency, whereas the three benzenesulfonamides **A3**, **A6**, and **M4** possess lipophilic substituents at the nitrogen and could be considered to be of the same family as other active hits, and compounds **B5**, **M1**, **M3**, **M6**, and **Me** have low negative inotropic activity and differ from each other.

The screening approach yielded excellent results with respect to the number of hits with significant inotropic activity, about 30% of the series, and with respect to the novelty of the scaffolds of the most promising compounds. In addition, even though **5b** possesses only inotropic activity without affecting the chronotropy and vasorelaxation as **DTZ** does, for these latter activities, unexpected interesting compounds were revealed. Compound **P1** also showed negative chronotropic activity, whereas compounds **B3**, **M4**, and **M8** showed vasorelaxant activity. The negative chronotropic potency of **P1** is interesting, being only 7-fold lower than that of diltiazem, whereas vasorelaxant activity greater than 50% was observed for compounds **B3**, **M4**, and **M8**, but only the value for **M8** was similar to that of diltiazem.

Further Functional Characterization of the Hits Found. To investigate the affinity of the most interesting hits for the binding site of **DTZ**, compounds **M2**, **M7**, **M8**, and **P1** were selected and analyzed together with **5b** and **DTZ**. Further functional tests were carried out for these selected compounds

Table 2. Cardiovascular Activity of the Enantiomers of **5b** and Tested Compounds in Comparison to that of References **5b** and Diltiazem

	% decrease (M ± SEM)		EC_{50} of inotropic negative potency		EC_{30} of chronotropic negative potency		vasorelaxant activity		
compd	negative inotropic activity[a] (**M** ± SEM)	negative chronotropic activity[b] (**M** ± SEM)	EC_{50}[c] (μM)	95% conf lim ($\times 10^{-6}$)	EC_{30}[c] (μM)	95% conf lim ($\times 10^{-6}$)	activity[d] (**M** ± SEM)	IC_{50}[c] (μM)	95% conf lim ($\times 10^{-6}$)
DTZ	78 ± 3.5[e]	94 ± 5.6[f]	0.79	0.70−0.85	0.07	0.064−0.075	88 ± 2.3	2.6	2.2−3.1
5b[g]	77 ± 1.7[h]	5 ± 0.2[i]	0.04	0.03−0.05			19 ± 0.9		
R(−) 5b	58 ± 3.4[h]	16 ± 0.8	0.07	0.04−0.08			11 ± 0.7		
S(+) 5b	47 ± 1.4[h]	15± 0.9[j]					7 ± 0.3		
A2	90 ± 4.0[f]	7 ± 0.6[f]	0.30	0.24−0.37			46 ± 2.1		
A3	98 ± 1.2[i]	6 ± 0.4	1.17	0.77−1.78			42 ± 2.4		
A4	66 ± 3.8	22 ± 1.1[f]	0.91	0.46−1.57			3 ± 0.2[j]		
A5	91 ± 1.9	4 ± 0.3[j]	0.36	0.27−0.48			33 ± 1.9		
A6	91 ± 3.6	14 ± 0.3	1.38	1.07−1.79			37 ± 2.4		
B2	81 ± 4.7	21 ± 1.4[f]	0.99	0.65−1.33			25 ± 1.7		
B3	73 ± 1.4[h]	5 ± 0.3	0.31	0.24−0.39			54 ± 3.1[k]	17.71	14.3−21.72
B4	84 ± 3.1	15 ± 0.8	0.73	0.51−1.03			28 ± 1.4		
B5	80 ± 5.1	22 ± 1.3[j]	2.28	1.98−2.61			23 ± 1.3		
B6	63 ± 1.7	13 ± 0.7[j]	0.90	0.59−1.36			9 ± 0.8[j]		
M1	71 ± 3.3[k]	7 ± 0.3[k]	2.55	1.80−3.61			9 ± 0.6		
M2	84 ± 0.7	13 ± 0.9	0.92	0.63−1.34			30 ± 2.4[j]		
M3	52 ± 1.3[i]	7 ± 0.6[i]	6.13	3.79−9.91			10 ± 0.7		
M4	92 ± 0.9[e]	5 ± 0.4	1.33	1.04−1.70			57 ± 1.6	25.10	15.28−32.05
M5	92 ± 3.4[k]	2 ± 0.1	1.00	0.66−1.43			29 ± 1.6		
M6	76 ± 2.5[k]	33 ± 2.4[i]	3.91	2.70−5.65			20 ± 1.3		
M7	61 ± 3.4	3 ± 1.5[j]	0.40	0.32−0.51			5 ± 0.4[j]		
M8	84 ± 1.6[f]	4 ± 0.2	0.31	0.22−0.42			74 ± 2.1	5.62	4.46−7.08
Me	78 ± 4.1	2 ± 0.1	7.51	5.98−9.44			16 ± 1.2		
P1	76 ± 4.0	64 ± 2.6[j]	0.313	0.20−0.48	0.48	0.32−0.59	19 ± 1.9		

[a] Activity: decrease in developed tension in isolated guinea-pig left atrium at 5×10^{-5} M, expressed as percent changes from the control ($n = 4-6$). The left atria were driven at 1 Hz. The 5×10^{-5} M concentration gave the maximum effect for most compounds. [b] Activity: decrease in atrial rate in guinea-pig spontaneously beating isolated right atria at 10^{-5} M, expressed as percent changes from the control ($n = 6-8$). The pretreatment heart rate ranged from 170 to 195 beats/min. The 10^{-5} M concentration gave the maximum effect for most compounds. [c] Calculated from log concentration−response curves (Probit analysis according to Litchfield and Wilcoxon[21] with $n = 6-8$). When the maximum effect was <50%, the inotropic EC_{50}, chronotropic EC_{30}, and IC_{50} values were not calculated. [d] Activity: percent inhibition of calcium-induced contraction on K^+-depolarized guinea-pig aortic strips at 10^{-4} M. The 10^{-4} M concentration gave the maximum effect for most compounds. [e] At 10^{-5} M. [f] At 5×10^{-6} M. [g] Taken from ref 13. [h] At 10^{-6} M. [i] At 10^{-4} M. [j] At 5×10^{-5} M. [k] At 5×10^{-4} M.

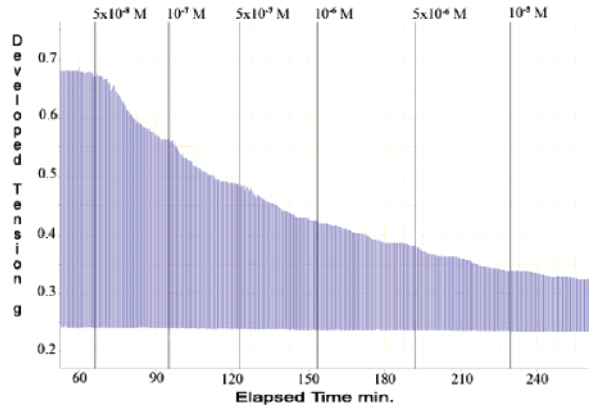

Figure 5. Guinea-pig left atrium driven at 1 Hz. A typical record of the decrease in the developed tension produced by **P1**. For details, see part B of the Experimental Section.

on isolated tissues, isolated organs (from guinea-pig), and cellular systems (binding in rat cardiomyocytes).

Guinea-pig isolated left papillary muscle was employed to assess the ventricular inotropic effect of the selected hits. Data are reported in section (a) of Table 3. All of the hits revealed an interesting negative inotropic activity in contrast to the inactive template **5b**. For **P1**, the activity is similar to that of **DTZ**, but the potency is 6-fold lower. **M8** is characterized by high activity and potency of the same order as that of **DTZ**, whereas for **M2** and **M7**, both activity and potency are largely higher than **DTZ**.

Thereafter, the cardiovascular profile of hits and references was extended to the guinea-pig isolated perfused heart, according to Langerdorff (see section (b) of Table 3). In this model, CEBs cause the decrease of maximal rate of the left ventricular pressure (+(d*P*/d*t*)max), the heart rate (HR), and the coronary perfusion pressure (CPP), together with a prolongation of atrioventricular conduction time (PR interval). Marked differences were observed between compound **5b**[13] and the hits and **DTZ**. Only the latter significantly influenced left ventricular contractile force, HR, and CPP. Concerning ECG parameters, **M8** is the hit with the most prolonged PR interval, even though it is of lower magnitude than that of **DTZ** and **5b**. On the contrary, **P1** is highly selective in its action because it does not influence the ECG at all.

Because the Ca^{2+} channel antagonists also have important inhibitory effects on vascular and nonvascular smooth muscle,[22] further investigations examined the relaxant activity on K^+ depolarized (80 mM) guinea-pig ileum longitudinal smooth muscle (GPILSM). Data are reported in section (c) of Table 3. When passing from aorta strips to nonvascular smooth muscle, **5b** was still inactive, whereas an increase of activity was registered for all of the hits, the most significant one occurring for **P1**. Even the potency, measured only for compounds with an efficacy more than 50%, significantly increased: **DTZ** gained 24-fold and **M8** 5-fold, whereas compound **P1** acted selectively on nonvascular smooth muscle with a significantly high efficacy.

It is well-known that the Ca^{2+} influx may occur through two distinct pathways, one activated by membrane depolarization and the other by receptor-mediated events.[23] The Ca^{2+} channel antagonists appear to discriminate between these two processes, preferentially inhibiting mechanical responses of Ca^{2+} influx through the voltage-dependent Ca^{2+} channels.[24] For hits and

Table 3. Further Functional Data for Some Selected Hits and References

	DTZ	5b	P1	M2	M7	M8
			(a) Negative inotropic potency on left ventricular papillary muscle			
% decrease[a]						
(M ± SEM)	82 ± 2.1	2 ± 0.1[b]	78 ± 3.4[c]	87 ± 2.4[d]	89 ± 0.7	93 ± 4.4
EC_{50}[e] (μM)	1.61		10.16	0.036	0.066	1.38
(95% c.l.) ($\times 10^{-6}$)	1.18−2.19		8.47−13.81	0.028−0.047	0.043−0.099	0.85−1.79
			(b) Cardiac activity on Langendorff preparation[f]			
+(d*P*/d*t*)max[g]	−59 ± 4.2	−3 ± 0.2	−12 ± 0.5	−31 ± 2.3	−17 ± 0.9	−6 ± 0.3
HR[h]	−25 ± 1.9	−14 ± 0.8	−12 ± 0.3	−4 ± 0.1	−14 ± 0.8	[n]
CPP[i]	−51 ± 3.1	−9 ± 0.5	−13 ± 0.2	[n]	−6 ± 0.2	+17 ± 1.1
PR[j]	+34 ± 2.2	+32 ± 1.6	[n]	+14 ± 1.0	+15 ± 1.1	+20 ± 1.3
			(c) Calcium channel antagonism on K^+-depolarized GPILSM			
% activity[k]						
(M ± SEM)	98 ± 1.5[d]	3 ± 0.2	89 ± 3.2[c]	99 ± 0.8	55 ± 0.6[b]	90 ± 0.7[l]
EC_{50}[e] (μM)	0.11		14.15	6.65	124.48	1.18
(95% c.l.) ($\times 10^{-6}$)	0.085−0.13		10.63−17.86	5.07−8.71	102.57−151.06	0.84−1.67
			(d) Calcium channel antagonist potency on GPILSM			
IC_{50}[e,m] (μM)	0.48	39.95	34.47	33.66	[n]	8.21
(95% c.l.) ($\times 10^{-6}$)	0.39−0.53	31.49−46.02	25.10−38.53	26.78−42.29		5.21−11.98

[a] Decrease in developed tension in isolated guinea-pig left ventricular papillary muscle driven at 1 Hz at 10^{-5} M. The 10^{-5} M concentration give the maximum effect for most compounds. [b] At 5×10^{-4} M. [c] At 5×10^{-5} M. [d] At 10^{-6} M. [e] Calculated from log concentration−response curves (Probit analysis according to Litchfield and Wilcoxon[21] with $n = 6-8$). When the maximum effect was <50%, the inotropic EC_{50} value was not calculated. [f] Percentage change of the basal value at the highest concentration tested (1 μM). Each value corresponded to the mean ± SEM. [g] +(d*P*/d*t*)max: maximal rate of the increase in left ventricular pressure. [h] HR: heart rate calculated from ECG signal. [i] CPP: coronary perfusion pressure. [j] PR: atrio-ventricular conduction time. [k] Percent inhibition of calcium-induced contraction on K^+-depolarized (80 mM) guinea-pig ileum longitudinal smooth muscle (GPILSM) at 10^{-4} M. The 10^{-4} M concentration gave the maximum effect for most compounds. [l] At 10^{-5} M. [m] Antagonist affinities are expressed as IC_{50}. IC_{50} is the concentration of antagonist causing 50% inhibition of the agonist maximal response in tonic contraction of guinea-pig ileum longitudinal smooth muscle induced by the muscarinic agonist carbachol. [n] Inactive.

reference compounds, the calcium channel antagonism was also determined as inhibition, induced by the muscarinic agonist carbachol, of the muscarinic receptor-mediated Ca^{2+}-dependent contraction of GPILSM at 10^{-5} M.[25,26] The results are reported in section (d) of Table 3 (for more details see Figure 8 in the Experimental Section). **M7** is inactive, and **DTZ** causes a significant decrease in the slow component of tonic response in GPILSM, whereas **M2**, **P1**, and **5b** display low potencies of the order of 10^{-5} M. In addition, although compound **M8** is about 17-fold less potent than **DTZ**, from these data, it emerges that compound **M8** is the most selective toward the membrane depolarization-induced contraction. The selectivity of these compounds is graphically represented in Figure 6.

Binding Profile of the Hits Found. For the series of selected candidates, binding assays on rat cardiomyocytes were carried out in order to establish their binding site. [^{3}H]Diltiazem (5 nM) was incubated with increasing concentrations (0.1 nM−100 μM) of the compounds as described in the Experimental Section. Data presented in Figure 7 reports the effects of the hits **M2**, **M3**, **M7**, **M8**, and **P1** on [^{3}H]diltiazem. Compound **M3** was added to double check the data because it showed a weak cardiovascular activity (Table 2), and therefore, it was expected to possess low binding affinity.

Compounds **P1**, **M2**, **M3**, **M7**, and **M8** affected the binding of [^{3}H]diltiazem, although in a different fashion. In fact, only **P1** caused a concentration-dependent inhibition of [^{3}H]diltiazem binding, with a pK_i of 5.52. In contrast, **M2**, **M3**, **M7**, and **M8** displayed a complex interaction with the benzothiazepine-binding site producing a small but reproducible stimulation of [^{3}H]diltiazem binding at lower concentrations, followed by partial inhibition at higher concentrations, as observed for **5b** (Figure 1 and Figure 7). The highest stimulation was observed with **M8** (24.8% of control at 10 nM), whereas the highest inhibition was displayed by **M2** (59.6% at 100 μM).

The findings presented in this study strongly suggest that **P1** is a novel CEB, which can inhibit L-type Ca^{2+} channel activity by interacting at the benzothiazepine-binding site in the cardiac

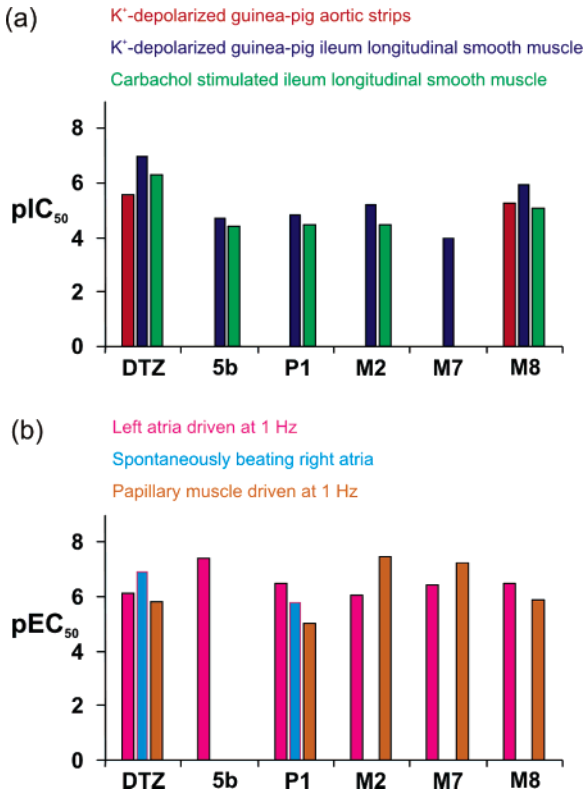

Figure 6. Potency of hits and reference compounds in different guinea-pig preparations.

α_1 subunit of the L-type Ca^{2+} channel. In fact, **P1** completely inhibited [^{3}H]diltiazem binding to rat cardiomyocytes, indicating a nonbenzothiazepine structure that can compete directly with diltiazem at the benzothiazepine-binding site. This is consistent with the effect presented here, which is produced by **P1** on cardiac and gut smooth muscle preparations where the molecule was shown to display the classical properties of a CEB. On the

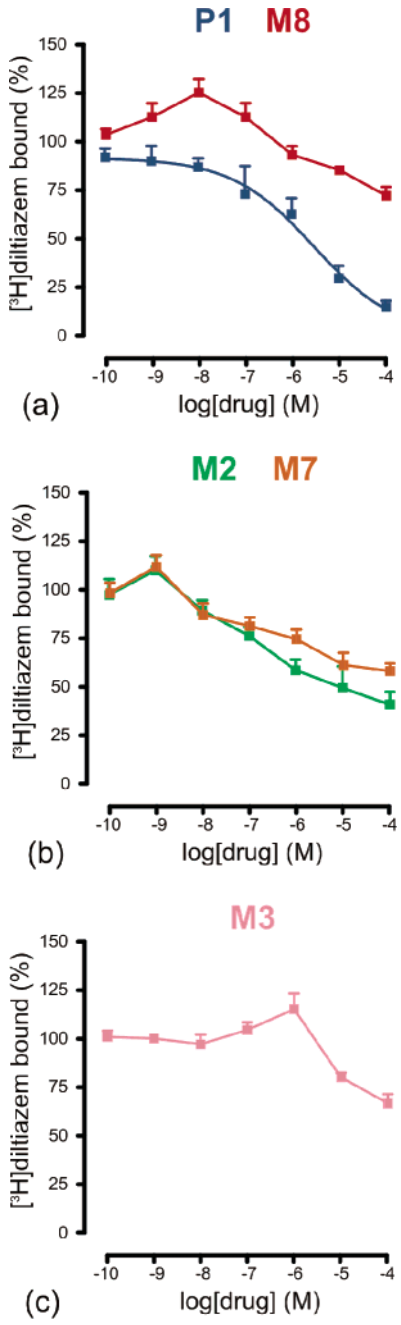

Figure 7. Effects of **P1**, **M2**, **M3**, **M7**, and **M8** on [^{3}H]diltiazem binding.

contrary, the minor effects displayed on vascular smooth muscle differentiated **P1** from diltiazem, suggesting that it might be classified as a unique CEB.

The mixed pattern of modulation characteristic of the hits **M2**, **M7**, and **M8** as well as **5b** is a preliminary indication that these compounds affect the benzothiazepine receptor at low concentrations by interacting at a distinct binding site, the occupation of which allosterically modulates diltiazem binding in a positive fashion. Clearly, these data indicate that **5b** and **M8** are the most interesting allosteric enhancers because [^{3}H]-diltiazem binding stimulation was observed under a wider range of concentrations (0.1 nM−1 μM and 0.1−100 nM, respectively) compared to those of the other hits.

However, at higher concentrations, these molecules interact directly at the benzothiazepine recognition site in the CEB−receptor complex, **M2** being the most active compound. Finally, the weak binding affinity displayed by **M3** is in agreement with its scarce cardiovascular activity, as previously hypothesized.

Conclusions

Virtual screening is increasingly gaining acceptance in the pharmaceutical industry as a cost-effective and timely strategy for analyzing very large chemical datasets. Successful applications of ligand-based virtual screening have been recently reported in the literature, as discussed in a recent review,[27] but even more are unpublished because of the proprietary nature of the molecules identified.[28] The results reported here confirm ligand-based virtual screening as an efficient approach to hit finding and support the conclusion that the novel computational procedure FLAP is a successful tool for LBVS.

Three novel chemotypes for L-type calcium channel antagonists were obtained: the benzenesulfonamide scaffold, varied successfully in different ways, the 3-phenyl-4-isoxazolecarboxylate, and the 4-phenyl-thiomorpholine-3,5-dione. All of these compounds were considered as hits, and some were investigated in more detail. All of them could be used to drive future synthetic and biological work.

Important findings were also obtained from HPLC, IR, and VCD methods because it was possible to illuminate the stereospecificity of the pharmacological action of compound **5b** because its *R*(−) form is more active. The relationship between this site and the diltiazem one needs to be investigated. As with **5b**, other hits also produced a biphasic effect, stimulating [^{3}H]diltiazem binding at low concentrations, and inhibiting it at higher concentrations. Conversely, **P1** caused a concentration-dependent inhibition of [^{3}H]diltiazem binding to rat cardiomyocytes. These results indicate that **P1** interacts directly at the benzothiazepine-binding site of the cardiac CEB−receptor complex, whereas **5b**, **M2**, **M7**, and **M8** show a complex interaction with the receptor.

Indeed, **P1** is a structurally unique CEB, rather selective toward the cardiac tissue. Its mechanism of action stems from its ability to interact with the CEB−receptor complex at a binding site heretofore recognized as being specific for molecules of the benzothiazepine chemical class.

Experimental Section

A. Enantiomers Separation. Apparatus. Analytical liquid chromatography was performed on a JASCO chromatograph equipped with a Rheodyne model 7725i 20 μL loop injector, PU-1580-CO_2 and PU-980 HPLC pumps, a Mod Jasco-975 single wavelength absorbance detector and a Jasco Mod 995-CD circular dichroism detector. Chromatographic data were collected and processed using Borwin software (Jasco Europe, Italy).

Semipreparative liquid chromatography was performed on a Waters chromatograph (Waters Associates) equipped with a Rheodyne model 7012 500 μL loop injector, a UV SpectroMonitor 4100 spectrophotometer, and a refractive index (Waters R401 detectors).

Chromatographic Procedures. The enantiomers of **5b** were resolved by semipreparative HPLC using (*R*,*R*)-DACH-DNB column (250 × 10 mm I.D.), *n*-hexane/dichloromethane 70/30 as eluent (flow rate 6 mL/min and T 25 °C), and UV, CD detectors at 270 nm. Sample **5b** was dissolved in the mobile phase (c = 55 mg/mL) and each injection was loaded with 50 μL (process yield 65%).

The enantiomeric excess and the UV and CD on-line spectra were determinated by analytical HPLC using an (*R*,*R*)-DACH-DNB column (250 × 4.6 mm I.D.) under the same conditions employed for semipreparative mode, except for flow rate (1 mL/min).

B. Functional Assays. The pharmacological profile of all compounds was tested on guinea-pig isolated left and right atria to evaluate their inotropic and chronotropic effects, respectively, and

on K^+-depolarized guinea-pig aortic strips to assess calcium antagonist activity. Guinea-pig isolated left papillary muscle was employed to assess the ventricular inotropic effect of **M2**, **M7**, **M8**, **P1**, and reference compounds **DTZ** and **5b**. Compounds were checked at increasing concentrations in order to evaluate the percentage decrease in developed tension on the isolated left atrium and papillary muscle driven at 1 Hz (negative inotropic activity), the percentage decrease in atrial rate on spontaneously beating right atrium (negative chronotropic activity), and the percentage inhibition of calcium-induced contraction on K^+-depolarized aortic strips (vasorelaxant activity).

According to Langendorff, the guinea-pig isolated perfused heart was used to assay the whole cardiac activity of compounds **M2**, **M7**, **M8**, **P1**, and references **DTZ** and **5b**. Compounds were checked at increasing concentrations to evaluate changes in left ventricular pressure (inotropic activity), heart rate (chronotropic activity), coronary perfusion pressure (coronary activity), and electrocardiogram (ECG) signal.

Data were analyzed using Student's *t*-test. The potency of drugs defined as EC_{50}, EC_{30}, and IC_{50} was evaluated from log concentration−response curves (Probit analysis using Litchfield and Wilcoxon or GraphPad Prism software)[21,29,30] in the appropriate pharmacological preparations. All data are presented as mean ± SEM.

1. Guinea-Pig Atrial Preparations. Female guinea-pigs (300−400 g) were sacrificed by cervical dislocation. After thoracotomy, the heart was immediately removed and washed by perfusion through the aorta with oxygenated Tyrode solution of the following composition (mM): 136.9 NaCl, 5.4 KCl, 2.5 $CaCl_2$, 1.0 $MgCl_2$, 0.4 $NaH_2PO_4 \times H_2O$, 11.9 $NaHCO_3$, and 5.5 glucose. The physiological salt solution (PSS) was buffered at pH 7.4 by saturation with 95% O_2/5% CO_2 gas, and the temperature was maintained at 35 °C. The following isolated guinea-pig heart preparations were used: spontaneously beating right atria and left atria driven at 1 Hz. For each preparation, the entire left and right atria were dissected from the ventricles, cleaned of excess tissue, hung vertically in a 15 mL organ bath containing the PSS continuously bubbled with 95% O_2/5% CO_2 gas at 35 °C at pH 7.4. Contractile activity was recorded isometrically by means of a force transducer (FT 0.3, Grass Instruments Corporation, Quincy, MA) using Power Lab software (AD-Instruments Pty., Ltd, Castle Hill, Australia). The left atria were stimulated by rectangular pulses of 0.6−0.8 ms duration and about 50% threshold voltage through two platinum contact electrodes in the lower holding clamp (Grass S88 Stimulator). The right atrium was in spontaneous activity. After the tissue was beating for several minutes, a length-tension curve was obtained, and the muscle was stretched to the length at which 90% of maximal force was developed. A stabilization period of 45−60 min was allowed before the atria were challenged by various agents. During the equilibration period, the bathing solution was changed every 15 min, and the threshold voltage was ascertained for the left atria. Atrial muscle preparations were used to examine the inotropic and chronotropic activity of the compounds (0.01, 0.05, 0.1, 0.5, 1, 5, 10, 50, and 100 μM), first dissolved in DMSO and then diluted with PSS. According to this procedure, the concentration of DMSO in the bath solution never exceeded 0.3%, a concentration which did not produce appreciable inotropic and chronotropic effects. During the generation of cumulative concentration−response curves, the next higher concentration of the compounds was added only after the preparation reached a steady state.

2. Guinea-Pig Left Papillary Muscle. The left ventricular papillary muscles were rapidly isolated from the heart and suspended in an organ bath (15 mL) containing modified Ringer solution of the following composition (mM): 135 NaCl, 5 KCl, 2 $CaCl_2$, 1 $MgCl_2$, 15 $NaHCO_3$ and 5.5 glucose, equilibrated with 95% O_2/5% CO_2 gas at pH 7.4 and maintained at 35 °C. The papillary muscles were driven through a pair of platinum electrodes (field stimulation) by square pulses (1 Hz, 5−7 ms, 50% threshold voltage). The tension that developed was recorded isometrically.

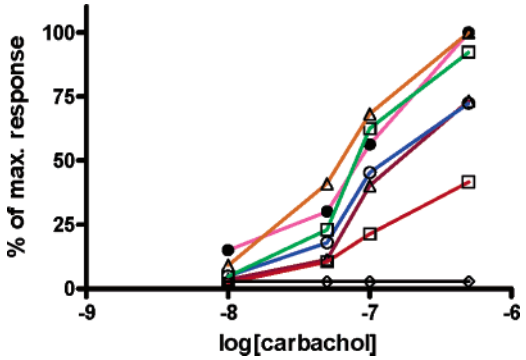

Figure 8. Guinea-pig ileum longitudinal smooth muscle antagonism of carbachol-induced contractions. Concentration−response curves for CHC were obtained before and after exposure to different drugs at 10 μM for 30 min. Each point is the mean (±SEM) of three observations. Legend: before exposure (●, pink line); after exposure to **DTZ** (◇, black line); **5b** (△, purple line); **M2** (□, green line); **M7** (△, orange line); **M8** (□, red line); **P1** (○, blue line).

The preparation was equilibrated for at least 60 min before the start of the experiment.

3. Guinea-Pig Aortic Strips and Ileum Longitudinal Smooth Muscle (GPILSM). The thoracic aorta and ileum were removed and placed in a Tyrode solution of the following composition (mM): 118 NaCl, 4.75 KCl, 2.54 $CaCl_2$, 1.20 $MgSO_4$, 1.19 KH_2PO_4, 25 $NaHCO_3$, and 11 glucose equilibrated with 95% O_2/5% CO_2 gas at pH 7.4. The vessel was cleaned of extraneous connective tissue. Two helicoidal strips (10 mm × 1 mm) were cut from each aorta beginning from the end most proximal to the heart. Vascular strips were then tied with surgical thread (6−0) and suspended in a jacketed tissue bath (15 mL) containing aerated PSS at 35 °C. Aortic strips were secured at one end to plexiglass hooks and connected via the surgical thread to a force displacement transducer (FT 0.3, Grass Instruments Corporation) for monitoring changes in isometric contraction. Aortic strips were subjected to a resting force of 1 g. The intestine was removed above the ileo-caecal junction. GPILSM segments of 2 cm length were mounted under a resting tension of 300−400 mg. Strips were secured at one end to a force displacement transducer (FT 0.3, Grass Instruments Corporation) for monitoring changes in isometric contraction and washed every 20 min with fresh PSS for 1 h. After the equilibration period, guinea-pig aortic strips were contracted by washing in PSS containing 80 mM KCl (equimolar substitution of K^+ for Na^+). When the contraction reached a plateau (about 45 min), various concentrations of the compounds (0.1, 0.5, 1, 5, 10, 50, 100, and 500 μM) were added cumulatively to the bath allowing for any relaxation to obtain an equilibrated level of force. The addition of the drug vehicle had no appreciable effect on K^+-induced contraction (DMSO for all compounds).

4. Calcium Channel Antagonist Activity on Guinea-Pig Ileum Longitudinal Smooth Muscle (GPILSM).[25] The intestine was removed above the ileo-caecal junction. Longitudinal smooth muscle segments of 2 cm length were mounted under a resting tension of 300−400 mg and maintained at 37 °C on a 15 mL jacketed organ bath containing oxygenated (100% O_2) PSS of the following composition (mM): 137 NaCl, 5.9 KCl, 2.6 $CaCl_2$, 1.2 $MgCl_2$, and 11.9 glucose buffered by 9 Hepes/NaOH to pH 7.4. The GPILSMs were equilibrated for 1 h, and PSS was changed every 15 min. Two successive control curves were constructed at 30 min intervals with carbachol (CHC). The isometric contractions were recorded with a force displacement transducer (FT 0.3, Grass Instruments Corporation). The muscle was washed with PSS and was allowed to reequilibrate. The calcium antagonist was added 30 min before the dose−response for CHC was determined. The drug-induced inhibition of contraction was expressed as a percentage of the control (Figure 8).

5. Guinea-Pig Isolated Perfused Heart According to Langendorff. Female guinea-pigs (300−400 g) were sacrificed by

cervical dislocation. The heart was quickly removed and rapidly perfused through the aorta at constant flow (11−12 mL min^{-1} g^{-1}) with a modified Krebs−Henselait solution with the following composition (mM): 128 NaCl, 4.7 KCl, 2.5 $CaCl_2$, 1.2 $MgSO_4$, 15 $NaHCO_3$, 1.2 KH_2PO_4, 11.1 glucose, and 2 Na-pyruvate, bubbled with a gas mixture (95% O_2/5% CO_2) (pH = 7.4−7.5) and maintained at 37 °C. A perfusion pressure of 50−60 mmHg was obtained at this flow rate. The addition of Na-pyruvate to the medium has been shown to confer to the isolated heart the same metabolic and functional features of the heart in situ.[31] A stabilization period of 30 min was given to the heart, under normal electrocardiogram (ECG) conditions, to keep the frequency of spontaneous beating hearts constant at 210 ± 3 beats min^{-1}. Surface ECG was recorded by means of two electrodes, one placed near the initial portion of the anterior intraventricular artery and the other on the left ventricular free wall. The main ECG intervals (*PR* = atrio-ventricular (AV) conduction time; *QRS* = intra-ventricular conduction time; *JT* = duration of ventricular depolarization) were measured. The drug-induced changes in conduction velocity of the AV node and the ventricular myocardium were calculated as changes in the reciprocal of the *PR* interval and *QRS* interval, respectively.[32] Heart contractility was measured, by means of an intraventricular latex balloon, as the positive peak of the first derivative of the left ventricular pressure as a function of time $[+(dP/dt)_{max}]$. Coronaric perfusion pressure (*CPP*) (mmHg) was measured to assess the change in coronary vessel resistance. The compounds were added at increasing concentrations (0.001, 0.01, 0.1, and 1 μM). During the building of concentration−response curves, the next higher concentration of the compounds was added only after the preparation reached a steady state (about 30 min). The potency of drugs, expressed as EC_{50} values, was evaluated from log concentration−response curves (n = 6−8)[33] in the appropriate pharmacological preparations. All data are presented as mean ± SEM.[33]

C. Binding Experiments. Cardiomyocytes Isolation. Single cardiac myocytes (CM) were isolated from male Sprague−Dawley rats (body weight 376 ± 12 g, n = 19, Charles River Italia, Como, Italy), injected with 500 U/100 g b.w. heparin i.p., anaesthetized with a mixture of Ketavet (Gellini, Italy) and Rompum (Bayer, Germany), decapitated, and bled.[34] After thoracotomy, the heart was rapidly removed, mounted on a micro-Langendorff apparatus, and perfused for 20 min at 37 °C with a nominally Ca^{2+}-free solution (low Ca^{2+} solution, LCS) of the following composition (mM): 120 NaCl, 10 KCl, 10 HEPES, 10 glucose, 1.2 $MgCl_2$, 1.2 KH_2PO_4, 5 Na-pyruvate, and 20 taurine at pH 7.2, equilibrated with 95% O_2/5% CO_2. The solution was then quickly changed to LCS complemented with 0.9 mg/mL of collagenase Type I (Sigma Chimica, Milan, Italy), 0.05 mg/mL of Dispase I (Roche Gmbh, Penzbeg, Germany), and 1.5 mg/mL of acid-free bovine serum albumin (Sigma Chimica, Milan, Italy) for 10 to 15 min. When the heart was soft, perfusion was stopped, and the tissue was chopped into small pieces and gently stirred in fresh LCS at room temperature. The cardiomyocytes that appeared in the supernatant were purified by centrifugation (5 min at 800*g*) and frozen at −80 °C until use. Pooled cells derived from at least two animals have been used for each binding experiment. Protein concentrations were estimated by using the method of Bradford[35] with BSA as the standard.

[^{3}H]Diltiazem Binding Assays. [^{3}H]Diltiazem binding assays were performed according to earlier methods[10,36] with some modifications. Aliquots of defrozen rat CM (200 μg) were incubated with ligands in 50 mM Tris buffer (pH 7.4) at 25 °C for 90 min in a final volume of 0.2 mL. In homologous competition curves, [^{3}H]-diltiazem (specific activity 85.5 Ci/mmol) was present at 20 nM in tubes containing increased concentrations of unlabeled diltiazem (5 nM−100 μM) and at 0.1−20 nM in tubes without the unlabeled ligand. In heterologous competition curves, fixed amounts of the tracer (5 nM) were displaced by increasing concentrations of several unlabeled ligands (0.1 nM − 100 μM). Incubation was terminated by rapid filtration on Whatman GF/B glass fiber filters (presoaked for at least 1 h in polyethyleneimmine 0.5%) and washed three times with 3 mL of ice-cold wash buffer. The filters were then placed in scintillation vials, 5 mL of liquid scintillation added, and the radioactivity measured in a LS5000CE β-counter (Beckman Instruments, Palo Alto, CA). Nonspecific binding was defined by means of 100 μM unlabeled diltiazem. All of the experiments were always run in triplicate.

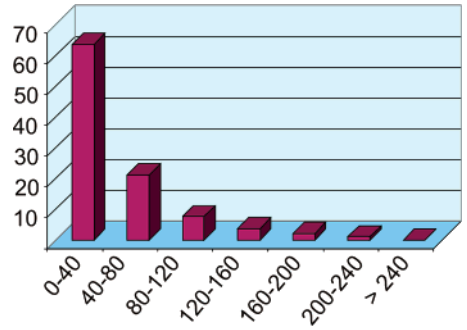

Figure 9. Histogram for the percentage of test compounds according to their FLAP scores.

Data Analysis. All of the experiments were performed by using rat cardiomyocytes, and all of the data are reported as mean ± SEM. Saturable binding constants relative to the binding of [^{3}H]-diltiazem were calculated by using the LIGAND program,[37,38] whereas the log of the half-maximal concentration (i.e., the pIC_{50} value) for the inhibition afforded by the derivatives was obtained by plotting specific binding (% of control) versus the log of the inhibitor concentration (M) and fitted with a non linear (sigmoidal) analysis.[29,30] The K_i was calculated according to the method of Cheng and Prusoff.[39]

D. Virtual Screening Procedure. Dataset. The dataset was assembled by collecting multimolecular files (in the formats SDF or multi-mol2) containing the 2D structures or 3D coordinates of the purchasable compounds. The overall amount was about 340 000 molecules, potential candidates for computational and biological screening. For the molecular structures obtained as SD files, the 3D coordinates were generated with an in-house software, which is also the basis for the FLAP conformational analysis. Compounds with undefined stereochemistry were initially provided as duplicates, and both configurations were used for the first steps of the screening. Later, for the FLAP similarity filter, each compound was ranked according to its best ranked configuration.

Pretreatment. The dataset was first processed to remove duplicates by encoding the 3D structures into canonical SMILES format by means of an in-house SMILES conversion program. In addition, salts, noncovalent compounds, and molecules containing atoms other than C, H, N, O, S, P, and halogens were excluded. The refinement of the dataset was completed by exclusion of compounds with MWs lower than 250 or higher than 700. Because the MW of the series of oxadiazolones (OD) ranged from approximately 250 to 600, the interval between 250 and 700 was used as MW filter. The upper edge was set to 700 in order to avoid the loss of interesting chemotypes as highly heavy compounds, perhaps due to the presence of heavy halogen atoms such as bromine or iodine. In addition, the elimination of compounds that were too large and bulky was guaranteed by the next filter, which would refer to size and shape.

Similarity Filter. The main step of the screening procedure was the similarity filter based on the novel procedure, FLAP.[18] FLAP was designed on the basis of the 4-point pharmacophoric method developed by Mason and co-workers[40] but contains several novelties and skills.

FLAP (fingerprints for ligands and proteins) provides a powerful engine for exploring the 3D-pharmacophore space of ligands and proteins. Starting from the GRID force field parametrization,[41,42] FLAP defines a 3D pharmacophore profile for ligands and proteins. Their common frame of reference allows ligand−ligand, ligand−protein, and protein−protein comparisons.

To build a molecular template, it is enough to run FLAP over the coordinate (KOUT) file of the molecule. Each atom, once

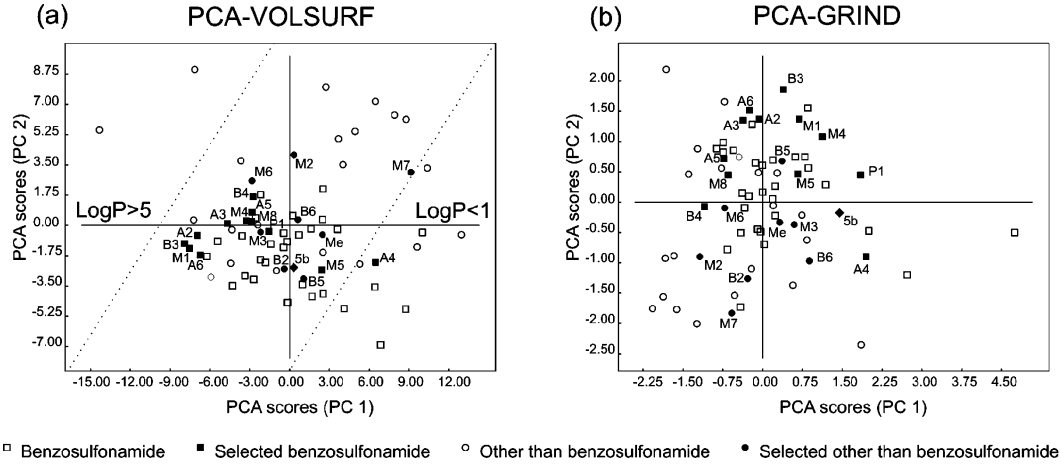

Figure 10. Score plots from PCA models based on VolSurf (a) and GRIND (b) molecular descriptors used to collect a balanced set.

classified in its corresponding GRID-type, which describes features such as hydrophobicity, hydrogen bond donor or/and acceptor, and positive or negative charge, is used as a site-point to build 4-point pharmacophores. The exhaustive combination of all of the atoms provides information about the 4-point pharmacophores, together with chirality, to be stored in an appropriate file.

The comparison of the test set molecule to the template was modulated by the following settings, reported according to their FLAP computational flags.

When pairing quadruplets of atoms, reported by their 3D coordinates, the pairwise distances are minimized. In the case of the equilibrium position reached , the comparison of this value with the tolerance ($b = 1$ Å) determines the 4-point pharmacophore to be included or excluded in the count.

Although a 4-point pharmacophore from the dataset compound is paired to the corresponding pharmacophore of the template, all of the remaining atoms of the test compound are fitted over the template molecule; some could lie out of the template molecular volume. The term c ($c = 0.40$) measures two times the percentage of atoms from the test molecule that are allowed to lie out of the template, in this case up to 20%.

The fitting of larger substrates is also modulated by the term d ($d = 2$ Å), which was specifically designed to expand the protein cavity of a fixed thickness to enable ligands to fit in. However, in the ligand-based approach, it is an expansion of the accessible volume described above (option c). The terms c and d tune the exclusion of nonsense solutions.

The FLAP procedure uses a conformational sampling when fitting the test molecule over the template: an on-the-fly generation of conformers is done at search time. The maximum number of rotatable bonds, equally distributed along the entire molecule ($r = 10$), and the maximum number of conformers that can be generated ($s = 100$) determine the conformational landscape. The method automatically selects the rotamers strategically located in the ligand in such a way that their modifications produce the maximum variation of the molecular atom positions. Once the rotamers have been selected, a random perturbation generates a population of possible rotamer solutions. Then, a quick evaluation of each conformation is performed on the basis of an internal steric contact check to reject poor or invalid ones.

At the end, for each test molecule, the procedure generates different conformations and, for each conformation, a series of different orientations. Each orientation contributes to the scoring of the paired conformation. Only the best conformation, in terms of the number of common 4-point pharmacophores in common with that of reference compound **5b**, defines the final score for the test molecule. The dataset compounds are then ranked according to their scores. The use of different orientations of the test molecule over the template guarantees the final score to be an effective measure of pharmacophore similarity, especially required in LBVS approaches where the active orientation of the molecular template is usually unknown.

The selectivity of the procedure is presented in Figure 9: about 85% of compounds lie in the first two bars with a score lower than 80, whereas 1% of compounds obtained a score greater than 200 and lie in the last two bars, and only 0.1% of the compounds lie in the last bar with a score greater than 240 and were selected for the further steps.

The FLAP software requires less than 1 s per conformer on a single CPU. On average, the throughput of FLAP/LBVS module with a maximum of 100 conformations for every molecule is about 5K molecules/processor/day on a linux machine equipped with a Pentium IV 3200 MHz prescott and 512 MB memory. The nature of computation is highly parallel, and an extension of the method to multiprocessors is planned for the near future.

Toxicity and Reactivity Filter. Toxic functional groups as well as reactive ones were removed following the suggestions of several authors.[19,20] Therefore, the presence of the following groups was used as criteria to skip compounds: five or more halogen atoms (but not two trihalo-methyl groups); two or more cyano or nitro groups; epoxide or azide; two or more aliphatic esters; 1,2-dicarbonyl group; sulfonate and phosphonate esters; aldehydes; acyl or sulfonyl halides; anhydrides; and heteroatom−heteroatom single bonds, when not in a cycle or linked to aromatic/olefinic systems.

In this manner, about half of the candidates (70 out of 150) passed the last filter and approached the final selection.

Final Selection of Candidates. Principal component analysis was performed to extract a small set of orthogonal factors describing data distribution in order to group molecules into clusters of related structures. Both the pharmacokinetic and pharmacodynamic profiles of candidates was inspected. VolSurf[43] was used for the former; the first PC of the model was highly related to the log P of compounds, and thereby, some candidates on the extremities were excluded because they were highly hydrophilic or highly lipophilic. Meanwhile, on the same set of candidates, the use of PCA over GRIND[44] allowed us to cluster compounds in order to select representatives and avoid redundancy. However, the overall distribution (especially between benzenesulfonamides and others) was maintained. In the end, 20 compounds were selected for purchasing. Figure 10 reports 70 virtual hits, together with **5b**, on the score plots derived from the PCA over VolSurf (a) and GRIND descriptors (b). Selected compounds are reported in black in Figure 10, where squares represent benzenesulfonamides and circles represent other compounds.

Acknowledgment. We thank Sigma-Aldrich for the generous gifts, all the other companies for special prices, and Dr. Massimo Baroni for his advice. This work was supported by grants from M.I.U.R.: PRIN-2005 “Chemistry, reactivity and biological activity of nitrogen- and/or oxygen- and/or sulphur-containing heterocycles”, PRIN-2003 “Design, synthesis and biological evaluation of new cardiovascular drugs”, and the University of Bologna.

Supporting Information Available: Details of the purchased compounds and details of ab initio calculations. This material is available free of charge via the Internet at http://pubs.acs.org.

References

(1) Grossman, E.; Messerli, F. H. Calcium Antagonists. *Prog. Cardiovasc. Dis.* **2004**, *47*, 34−57.

(2) Striessnig, J.; Grabner, M.; Mitterdorfer, J.; Hering, S.; Sinnegger, M. J.; Glossmann, H. Structural basis of drug binding to L-type Ca^{2+} channels. *Trends Pharmacol. Sci.* **1998**, *19*, 108−115.

(3) Materson, B. J. Calcium channel blockers. Is it time to split the lump? *Am. J. Hypertens.* **1995**, *8*, 325−329.

(4) Glossmann, H.; Striessnig, J. Molecular properties of calcium channels. *Rev. Physiol. Biochem. Pharmacol.* **1990**, *114*, 1−105.

(5) Brauns, T.; Prinz, H.; Kimball, S. D.; Haugland, R. P.; Striessnig, J.; Glossmann, H. L-type calcium channels: Binding domains for dihydropyridines and benzothiazepines are located in close proximity to each other. *Biochemistry* **1997**, *36*, 3625−3631.

(6) Buckley, M.; Grant, S.; Goa, K.; McTavish, D.; Sorkin, E. Diltiazem: A reappraisal of its pharmacological properties and therapeutic use. *Drugs* **1990**, *39*, 757−806.

(7) Kawai, C.; Konishi, T.; Matsuyama, E.; Okazaki, H. Comparative effects of three calcium antagonists, diltiazem, verapamil and nifedipine, on the sinoatrial and atrioventricular nodes. *Circulation* **1981**, *82*, 1962−1972.

(8) Zhou, S.; Chan, E.; Lim, L. Y.; Boelsterli, U. A.; Li, S. C.; Wang, J.; Zhang, Q.; Huang, M.; Xu, A. Therapeutic drugs that behave as mechanism-based inhibitors of cytochrome P450 3A4. *Curr. Drug Metab.* **2004**, *5*, 415−442.

(9) Floyd, D. M.; Kimball, S. D.; Krapcho, J.; Das, J.; Turk, C. F.; Moquin, R. V.; Lago, M. W.; Duff, K. J.; Lee, V. G.; White, R. E.; Ridgewell, R. E.; Moreland, S.; Brittain, R. J.; Normandin, D. E.; Hedberg, S. A.; Cucinotta, G. G. Benzazepinone calcium channel blockers. 2. Structure−activity and drug metabolism studies leading to potent antihypertensive agents. Comparison with benzothiazepinones. *J. Med. Chem.* **1992**, *35*, 756−772.

(10) Zobrist, R. H.; Mecca, T. E. [^{3}H]TA-3090, a selective benzothiazepine-type calcium channel receptor antagonist: In vitro characterization. *J. Pharmacol. Exp. Ther.* **1990**, *253*, 461−465.

(11) Hagiwara, M.; Adachi-Akahane, S.; Nagao, T. High-affinity binding of [^{3}H]DTZ323 to the diltiazem-binding site of L-type Ca^{2+} channels. *Eur. J. Pharmacol.* **2003**, *466*, 63−71.

(12) Budriesi, R.; Cosimelli, B.; Ioan, P.; Lanza, C. Z.; Spinelli, D.; Chiarini, A. Cardiovascular characterization of [1,4]thiazino[3,4-*c*]-[1,2,4]oxadiazol-1-one-derivatives: Selective myocardial calcium channel modulators. *J. Med. Chem.* **2002**, *45*, 3475−3481.

(13) Budriesi, R.; Carosati, E.; Chiarini, A.; Cosimelli, B.; Cruciani, G.; Ioan, P.; Spinelli, D.; Spisani, R. A new class of selective myocardial calcium channel modulators. 2. The role of the acetal chain in oxadiazol-3-one derivatives. *J. Med. Chem.* **2005**, *48*, 2445−2456.

(14) Garcia, M. L.; King, V. F.; Siegl, P. K.; Reuben, J. P.; Kaczorowski, G. J. Binding of Ca^{2+} entry blockers to cardiac sarcolemmal membrane vesicles. Characterization of diltiazem-binding sites and their interaction with dihydropyridine and aralkylamine receptors. *J. Biol. Chem.* **1986**, *261*, 8146−8157.

(15) (a) Stephens, P. J.; Devlin, F. J. Determination of the structures of chiral molecules using ab initio vibrational circular dichroism spectroscopy. *Chirality* **2000**, *12*, 172−179. (b) Stephens, P. J.; Devlin, F. J.; Aamouche, A. Determination of the Structures of Chiral Molecules Using Vibrational Circular Dichroism Spectroscopy. In *Chirality: Physical Chemistry;* Hicks, J. M., Ed.; ACS Symposium Series; American Chemical Society: Washington, DC, 2002; pp 18−33. (c) Stephens, P. J. Vibrational circular dichroism spectroscopy: A New Tool for the Stereochemical Characterisation of Chiral Molecules. In *Computational Medicinal Chemistry for Drug Discovery*; Bultinck, P., de Winter, H., Langenaecker, W., Tollenaere, J., Eds.; Dekker: New York, 2003; pp 699−725. (d) Cere, V.; Peri, F.; Pollicino, S.; Ricci, A.; Devlin, F. J.; Stephens, P. J.; Gasparrini, F.; Rompietti, R.; Villani, C. Synthesis, chromatographic separation, VCD spectroscopy and ab initio DFT studies of chiral thiepane tetraols. *J. Org. Chem.* **2005**, *70*, 664−669.

(16) http://www.molsoft.com/screening.html.

(17) Oprea, T. I.; Gottfries, J. Chemography: The art of navigating in chemical space. *J. Comb. Chem.* **2001**, *3*, 157−166.

(18) Perruccio, F.; Mason, J. S.; Sciabola, S.; Baroni, M. FLAP: 4-Point Pharmacophore Fingerprints from GRID. In *GRID-Based Molecular Interaction Field in Cheminformatics and Drug Design*; Cruciani, G., Ed.; Wiley-VCH: Weinheim, Germany, 2005; pp 83−102.

(19) Rishton, G. M. Reactive compounds and in vitro false positive in HTS. *Drug Discovery Today* **1997**, *2*, 382−384.

(20) Olah, M. M.; Bologa, C. G.; Oprea, T. I. Strategies for compound selection. *Curr. Drug Discovery Technol.* **2004**, *1*, 211−220.

(21) Tallarida, R. J.; Murray, R. B. *Manual of Pharmacologic Calculations with Computer Programs*, 2nd ed.; Springer-Verlag: New York, 1987.

(22) Bolger, G. T.; Genco, P.; Klockowski, R.; Luchowski, E.; Siegel, H.; Janis, R. A.; Triggle, A. M.; Triggle, D. J. Characterization of binding of the Ca^{2+} channel antagonist, [^{3}H]nitrendipine, to guinea-pig ileal smooth muscle. *J. Pharmacol. Exp. Ther.* **1983**, *225*, 291−309.

(23) Bolton, T. B. Mechanism of action of transmitters and other substances on smooth muscle. *Physiol. Rev.* **1979**, *59*, 606−718.

(24) Triggle, D. J. Calcium Antagonists: Basic Chemical and Pharmacological Aspects. In *New Perspectives on Calcium Antagonists*; Weiss, G. B., Ed.; American Physiological Society, Bethesda, MD, 1981; pp 1−18.

(25) Dagnino, L.; Li-Kwong-Ken, M. C.; Wolowyk, M. W.; Triggle, C. R.; Knaus, E. E. Synthesis and calcium channel antagonist activity of dialkyl 4-(dihydropyridinyl)-1,4-dihydro-2,6-dimethyl-3,5-pyridinedicarboxylates. *J. Med. Chem.* **1987**, *30*, 640−646.

(26) Unno, T.; Matsuyama, H.; Sakamoto, T.; Uchiyama, M.; Izumi, Y.; Okamoto, H.; Yamada, M.; Wess, J.; Komori, S. M(2) and M(3) muscarinic receptor-mediated contractions in longitudinal smooth muscle of the ileum studied with receptor knockout mice. *Br. J. Pharmacol.* **2005**, *146*, 98−108.

(27) Oprea, T. I.; Matter, H. Integrating virtual screening in lead discovery. *Curr. Opin. Chem. Biol.* **2004**, *8*, 349−358.

(28) Pirard, B.; Brendel, J.; Peukert, S. The discovery of Kv1.5 blockers as a case study for the application of virtual screening approaches. *J. Chem. Inf. Model.* **2005**, *45*, 477−485.

(29) Motulsky, H.; Christopoulos, A. Fitting models to biological data using linear and non linear regression, 2003, http://www.graphpad.com.

(30) Motulsky, H. Statistic guide: Statistical analysis for laboratory and clinical research: A pratical guide to curve fitting, 2003, http://www.graphpad.com.

(31) Bunger, R. F. J.; Haddy, A.; Querengasser, E.; Gerlach, E. An isolated guinea-pig heart preparation with in vivo like feature. *Pflügers. Arch.* **1975**, *353*, 317−326.

(32) Bova, S.; Cargnelli, G.; D′Amato, E.; Forti, S.; Yang, Q.; Trevisi, L.; Debetto, P.; Cima, L.; Luciani, S.; Padrini, R. Calcium-antagonist effects of norbormide on isolated perfused heart and cardiac myocytes of guinea-pig: A comparison with verapamil. *Br. J. Pharmacol.* **1997**, *120*, 19−24.

(33) *GraphPad Prism 3.02*; GraphPad Software, Inc.; http://www.graphpad.com

(34) Matucci, R.; Ottaviani, M. F.; Barbieri, M.; Cerbai, E.; Mugelli, A. Protective effect of darodipine, a calcium antagonist, on rat cardiomyocytes against oxygen radical-mediated injury. *Br. J. Pharmacol.* **1997**, *122*, 1353−1360.

(35) Bradford, M. M. A rapid and sensitive method for the quantitation of microgram quantities of protein utilizing the principle of protein-dye binding. *Anal. Biochem.* **1976**, *72*, 248−254.

(36) Wei, X. Y.; Rutledge, A.; Triggle, D. J. Voltage-dependent binding of 1,4-dihydropyridine Ca^{2+} channel antagonists and activators in cultured neonatal rat ventricular myocytes. *Mol. Pharmacol.* **1989**, *35*, 541−552.

(37) Munson, P. J.; Rodbard, D. LIGAND: A versatile computerized approach for the characterization of ligand-binding systems. *Anal. Biochem.* **1980**, *107*, 220−239.

(38) Unnerstall, J. R. Computer Analysis of Binding Data. In *Methods in Neurotransmitter receptor analysis*; Yamamura, H. I., Enna, S. J., Kuhar, M. J., Eds.; Raven Press: New York, 1990; pp 37−68.

(39) Cheng, Y. C.; Prusoff, W. H. Relationship between the inhibition constant (K_i) and the concentration of inhibitor which causes 50% inhibition (IC_{50}) of an enzymatic reaction. *Biochem. Pharmacol.* **1973**, *22*, 3099−3108.

(40) Mason, J. S.; Morize, I.; Menard, P. R.; Cheney, D. L.; Hulme, C.; Labaudiniere, R. F. New 4-point pharmacophore method for molecular similarity and diversity applications: Overview of the method and applications, including a novel approach to the design of combinatorial libraries containing privileged substructures. *J. Med. Chem.* **1999**, *42*, 3251−3264.

(41) Goodford, P. J. A Computational procedure for determining energetically favorable binding sites on biologically important macromolecules. *J. Med. Chem.* **1985**, *28*, 849−857.

(42) Carosati, E.; Sciabola, S.; Cruciani, G. Hydrogen bonding interactions of covalently bonded fluorine atoms: From crystallographic data to a new angular function in the GRID force field. *J. Med. Chem.* **2004**, *47*, 5114−5125.

(43) *VolSurf 4.1*; Molecular Discovery, Ltd.; http://www.moldiscovery.com.

(44) *Almond 3.3*; Molecular Discovery, Ltd.; http://www.moldiscovery.com.

JM0604373